.

Inductively coupled plasma etch damage in (-201) Ga_2O_3 Schottky diodes

Jiancheng Yang, Shihyun Ahn, F. Ren, Rohit Khanna, Kristen Bevlin, Dwarakanath Geerpuram, S. J. Pearton, and A. Kuramata

Citation: Appl. Phys. Lett. **110**, 142101 (2017); doi: 10.1063/1.4979592
View online: http://dx.doi.org/10.1063/1.4979592
View Table of Contents: http://aip.scitation.org/toc/apl/110/14
Published by the American Institute of Physics

Articles you may be interested in

High pulsed current density β-Ga2O3 MOSFETs verified by an analytical model corrected for interface charge
Appl. Phys. Lett. **110**, 143505143505 (2017); 10.1063/1.4979789

Tuning the thickness of exfoliated quasi-two-dimensional β-Ga2O3 flakes by plasma etching
Appl. Phys. Lett. **110**, 131901131901 (2017); 10.1063/1.4979028

1-kV vertical Ga2O3 field-plated Schottky barrier diodes
Appl. Phys. Lett. **110**, 103506103506 (2017); 10.1063/1.4977857

Schottky barrier diode based on β-Ga2O3 (100) single crystal substrate and its temperature-dependent electrical characteristics
Appl. Phys. Lett. **110**, 093503093503 (2017); 10.1063/1.4977766

Quasiparticle self-consistent GW band structure of β-Ga2O3 and the anisotropy of the absorption onset
Appl. Phys. Lett. **110**, 132103132103 (2017); 10.1063/1.4978668

150 mW deep-ultraviolet light-emitting diodes with large-area AlN nanophotonic light-extraction structure emitting at 265 nm
Appl. Phys. Lett. **110**, 141106141106 (2017); 10.1063/1.4978855

Fearful for the future of science?
Sign up for FREE FYI emails.
AIP | American Institute of Physics

Inductively coupled plasma etch damage in (-201) Ga_2O_3 Schottky diodes

Jiancheng Yang,[1] Shihyun Ahn,[1] F. Ren,[1] Rohit Khanna,[2] Kristen Bevlin,[2] Dwarakanath Geerpuram,[2] S. J. Pearton,[3] and A. Kuramata[4]
[1]*Department of Chemical Engineering, University of Florida, Gainesville, Florida 32611, USA*
[2]*Plasma-Therm, Saint Petersburg, Florida 33716, USA*
[3]*Department of Materials Science and Engineering, University of Florida, Gainesville, Florida 32611, USA*
[4]*Tamura Corporation and Novel Crystal Technology, Inc., Sayama Saitama 350-1328, Japan*

(Received 11 February 2017; accepted 21 March 2017; published online 3 April 2017)

Bulk, single-crystal Ga_2O_3 was etched in BCl_3/Ar inductively coupled plasmas as a function of ion impact energy. For pure Ar, the etch rate (R) was found to increase with ion energy (E) as predicted from a model of ion enhanced sputtering by a collision-cascade process, R $\propto(E^{0.5} - E_{TH}^{0.5})$, where the threshold energy for Ga_2O_3, E_{TH}, was experimentally determined to be ∼75 eV. When BCl_3 was added, the complexity of the ion energy distribution precluded, obtaining an equivalent threshold. Electrically active damage introduced during etching was quantified using Schottky barrier height and diode ideality factor measurements obtained by evaporating Ni/Au rectifying contacts through stencil masks onto the etched surfaces. For low etch rate conditions (∼120 Å min^{-1}) at low powers (150 W of the 2 MHz ICP source power and 15 W rf of 13.56 MHz chuck power), there was only a small decrease in reverse breakdown voltage (∼6%), while the barrier height decreased from 1.2 eV to 1.01 eV and the ideality factor increased from 1.00 to 1.06. Under higher etch rate (∼700 Å min^{-1}) and power (400 W ICP and 200 W rf) conditions, the damage was more significant, with the reverse breakdown voltage decreasing by ∼35%, the barrier height was reduced to 0.86 eV, and the ideality factor increased to 1.2. This shows that there is a trade-off between the etch rate and near-surface damage. *Published by AIP Publishing.*
[http://dx.doi.org/10.1063/1.4979592]

Ga_2O_3 is attracting attention for its application in solar-blind UV light-emitters, gas sensors, and power electronics.[1–7] The β-polytype is the most stable, exhibits wide bandgap (∼4.8 eV), and can be grown in the form of very high quality bulk crystals and epitaxial films.[1–11] Bulk substrates up to 4 in. in diameter with the absence of twin boundaries have been demonstrated,[1] leading to variety of electronic devices such as Schottky diodes, enhancement-mode fin field effect transistors, and metal-oxide field effect transistors with impressive performance.[12–21] There is still much work to be done to develop processing modules for this material and to understand the effects of these processes on the electrical properties. While numerous wet etchants have been reported for Ga_2O_3, including HNO_3/HCl and HF,[22,23] little is known about its dry etching characteristics and the associated mechanisms and effects on the electrical properties of the material. Some initial results have appeared on reactive ion and inductively coupled plasma (ICP) etching in SF_6 and Cl_2/BCl_3 mixtures,[24,25] while plasma-induced damage from Ar[24] was found to induce measurable changes in absorption properties. One of the best ways to quantify the electrical damage due to dry etching is to look at changes in the barrier height of Schottky diodes fabricated on the etched surface.[26] Schottky contact technology is relatively well-established for Ga_2O_3.[27,28]

In this letter, we report on an investigation of the etching characteristics of high-quality, bulk single-crystal Ga_2O_3 in inductively coupled plasmas (ICPs) of BCl_3/Ar, a common plasma chemistry for III–V compound semiconductors and electronic oxides.[29] BCl_3 is a Lewis acid that is effective in reacting with oxides and it getters water vapor. The etching mechanism was investigated by varying the ion impact energy and the resulting effects on the barrier height and ideality factor of Schottky diodes deposited onto the etched surface of the Ga_2O_3.

The starting sample was a bulk β-phase Ga_2O_3 single crystal with (-201) surface orientation (Tamura Corporation, Japan) grown by the edge-defined film-fed growth method. Hall Effect measurements showed that the sample was unintentionally n-type with an electron concentration of $\sim3\times10^{17}\,cm^{-3}$. Full-area back Ohmic contacts were created using Ti/Au (20 nm/80 nm) deposited by e-beam evaporation. Linear current-voltage behavior was obtained without the need for a rapid annealing step. Photoresist masked and unmasked samples were exposed to $15BCl_3/5Ar$ discharges (where the numbers represent the respective gas flows in standard cubic centimeters per minute) in a Plasma-Therm Versaline ICP reactor. The 2 MHz power applied to the 3-turn ICP source was varied from 150 to 400 W, while the rf (13.56 MHz) chuck power was varied from 15 to 200 W. The power controls the ion density, while the latter controls the ion energy. Over the rf power range investigated, the dc self-bias on the sample electrode varied from −10 V to −146 V. The electrode setup uses mechanical clamping on the periphery of the wafer, with the region between the electrode and wafer back side being enveloped with He (maintaining a 4 torr pressure) sealed behind the wafer to get good heat transfer between the wafer and electrode even in a high bias process. Then, the heat exchanger temperature of 25 °C can be maintained efficiently on the sample, helping to prevent any resist reticulation. Etch rates were obtained from stylus profilometry measurements of the patterned samples. The blanket samples

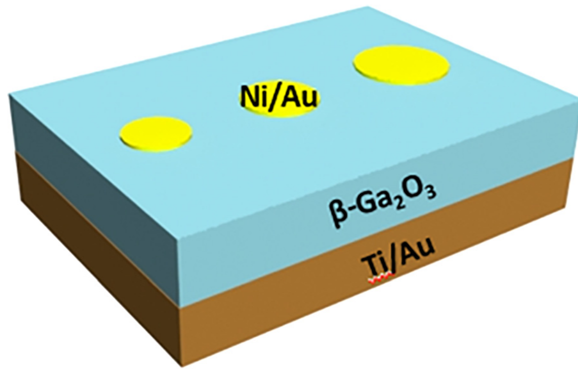

FIG. 1. Schematic of Ni/Au Ga_2O_3 Schottky diodes on dry etched surfaces.

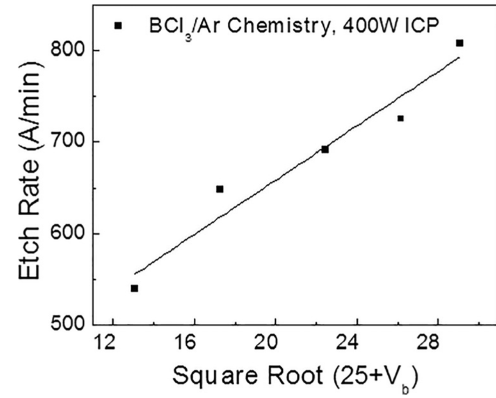

FIG. 2. The etch rate of Ga_2O_3 in BCl_3/Ar plasmas as a function of the average ion kinetic energy (plasma potential of +25 V minus the measured dc bias voltage).

with full area back contacts were used for electrical measurements since we did not want interference from resist removal processes to affect the etched surface. Schottky contacts were prepared on the front sides of the unmasked samples by e-beam deposited contacts Ni/Au (20 nm/80 nm) through a stencil mask. Figure 1 shows a schematic of the completed diodes. The forward and reverse current-voltage (I–V) characteristics were recorded at 25 °C using an Agilent 4145B parameter analyzer. Three diodes were measured for each condition, and the results were found to be within 5% in terms of breakdown voltage, a testament to the excellent uniformity of the substrates.

We were able to identify two etch regimes with high and low rates. These are summarized in Table I. With discharge gas compositions of $15BCl_3$ /5Ar and conditions of relatively high ICP source power (400 W) and rf chuck power (200 W), the etch rate was 692 Å min^{-1}, the highest yet reported for Ga_2O_3. Note that photoresist is not degraded by these conditions, and they represent practical plasma parameters for device fabrication processes. At lower source power (150 W) and rf power (15 W), the etch rate was 121 Å min^{-1}.

To establish the mechanism for etching, the etch rates were obtained for different plasma compositions and chuck biases. Figure 2 shows the Ga_2O_3 etch rate as a function of the substrate bias, V_b in BCl_3/Ar discharges. The ICP source power was held constant at 150 W for these runs. The x-axis is plotted as the square root of the average ion energy, which is the plasma potential of ∼25 V minus the dc self-bias. A commonly accepted model for an etching process occurring by ion-enhanced sputtering in a collision-cascade process predicts that the etch rate will be proportional to $E^{0.5}$-$E_{TH}{}^{0.5}$, where E is the ion energy and E_{TH} is the threshold energy.[30] Therefore, a plot of etch rate versus $E^{0.5}$ should be a straight line with an x-intercept equal to E_{TH}. The BCl_3/Ar data would indicate negative activation energy, but this is an artifact of the complexity of the ion energy distribution in that chemistry, as reported in detail previously.[31–33] In the case of Ar, which is a pure ion-assisted etch mechanism, the value of E_{TH} was ∼75 eV. We use the Ar-only etching simply to derive the threshold energy for initiation of etching. This is not a practical etch process since the selectivity to mask materials is low, and there will be maximum ion-induced damage.

To understand the relative magnitude of electrically active damage induced by different etch conditions, the I–V characteristics were recorded. The basic current transport processes in Schottky contacts will be thermionic emission, which generally dominates for moderately doped, high-mobility semiconductors.[33] The I–V characteristic is then given by the relation[33]

$$I = I_S \exp(eV/nkT)\left[1 - \exp\left(-\frac{eV}{nkT}\right)\right],$$

where I_S is the saturation current given by

$$I_S = AA^*T^2 \exp(\varphi_b)/kT,$$

where A is the contact area, A^* is the effective Richardson constant (33.7 A cm^{-2} K^{-2} for Ga_2O_3),[27] Φ_B is the effective barrier height, n is the ideality factor, *e* is the electronic charge, k is Boltzmann's constant, and T is the absolute temperature. If the current flow is dominated by thermionic emission, then the ideality factor *n* should be close to unity, with a small increase from unity due to the image force effect.[27,33,34]

Figure 3 shows the reverse I–V characteristics of the diodes for different ICP and rf powers and etch times, corresponding to the high rate and low rate etching conditions, respectively. Note that the low rate conditions with a low

TABLE I. Schottky barrier height and diode ideality factor for Ga_2O_3 under different ICP conditions of 15 BCl_3/5 Ar discharges. Low etch A and B refer to different times (10 and 20 mins, respectively) under low etch rate conditions. The high etch rate condition was also carried out for 10 min.

Sample	ICP Power (W)	RF Power (W)	Etch Rate (Å/min)	Schottky Barrier Height (eV)	Ideality Factor
Reference	0	0	0	1.20	1.00
High etch	400	200	692	0.86	1.20
Low etch A	150	15	121	1.01	1.06
Low etch B	150	15	121	1.02	1.08

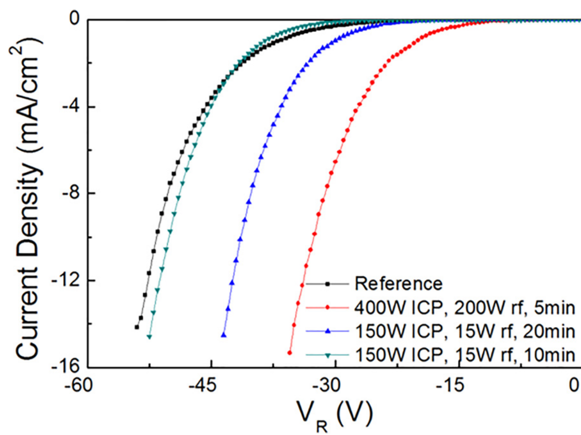

FIG. 3. Reverse I–V characteristics of Ga_2O_3 diodes on surfaces dry etched under different conditions of ICP and rf power and etch time.

source and chuck powers for an etch time of 10 min lead to a decrease of ∼6% in reverse breakdown voltage compared to the unetched reference sample. If the etching under these conditions continues for twice as long (20 min), the degradation in reverse breakdown voltage is more severe, indicating that the ion-induced damage accumulates. The fast etch rate conditions with a high source and chuck power lead to a decrease in the breakdown voltage of ∼35%. The degradation in reverse characteristics is common in semiconductors and is ascribed to introduction of point defects that act as generation-recombination centers and traps for free carriers (see Ref. 35, pp. 309–360).

Figure 4 shows the forward I–V characteristics for the same etching conditions as Figure 3. For extraction of the effective barrier height from the I–V characteristics of our Schottky diodes, we fitted the linear portions that obeyed the ideal thermionic-emission behavior. We did not observe the significant hysteresis effects in these diodes, with measurements standardized to repeat the I–V sweep at 1 min intervals. The shift in the I–V curves is due to contributions from leakage current contributions from both the bulk space-charge region and the surface. Surface leakage can be more significant in diodes containing plasma-induced damage.[36] Table I also summarizes the resulting values. The reference values of Φ_B of 1.07 eV and n = 1.00 (these values are

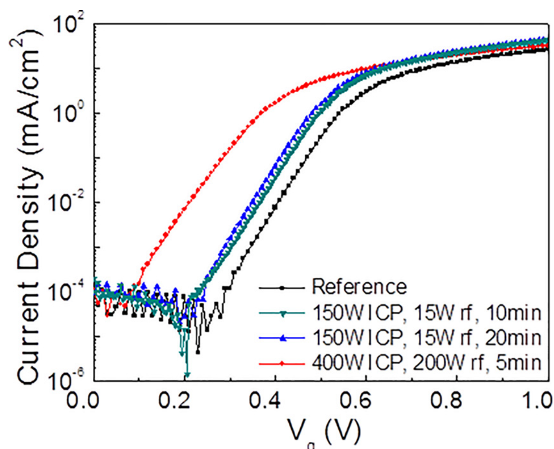

FIG. 4. Forward I–V characteristics of Ga_2O_3 diodes on surfaces dry etched under different conditions of ICP and rf power and etch time.

comparable to previous results for Ni[7,37]) are degraded by the etching processes. For the high etch rate condition, Φ_B decreases to 0.86 eV and n increases to 1.20. The low rate etch conditions lead to smaller amounts of degradation in both the barrier height and ideality factor. This suggests that an obvious strategy when needing to etch large distances in Ga_2O_3 while maintaining the electrical quality of the final surface is to initially employ high power conditions and then reduce these powers as the endpoint is reached. This type of process where initial high ion energy (and high rate process) is followed by "soft landing" near the end of the etch is utilized in other wide-bandgap semiconductors such as high rate SiC etching and has been found to be a solution for preventing the surface damage, notching, and micro-trenching near the bottom of sidewalls and on the wafer surface. Of course, annealing or wet etch cleanup of damaged surfaces can also be employed to recover a pristine surface after plasma etching.

In summary, dry etching processes for Ga_2O_3 have been identified with a high rate in one case and low amounts of damage in the other. The ion energy threshold for etching Ga_2O_3 under purely physical conditions was obtained. For BCl_3/Ar, the etch rate increases with ion energy as predicted from an ion-assisted chemical sputtering process.

The work at UF was partially supported by HDTRA (Grant No. 1-17-1-001). Part of the work at Tamura was supported by "The research and development project for innovation technique of energy conservation" of the New Energy and Industrial Technology Development Organization (NEDO), Japan. We also thank Dr. Kohei Sasaki from Tamura Corporation for fruitful discussions.

[1]A. Kuramata, K. Koshi, S. Watanabe, Y. Yamaoka, T. Masui, and S. Yamakoshi, Jpn. J. Appl. Phys., Part 1 **55**, 1202A2 (2016).
[2]M. J. Tadjer, M. A. Mastro, N. A. Mahadik, M. Currie, V. D. Wheeler, J. A. Freitas, Jr., J. D. Greenlee, J. K. Hite, K. D. Hobart, C. R. Eddy, Jr., and F. J. Kub, J. Electr. Mater. **45**, 2031 (2016).
[3]M. Higashiwaki, K. Sasaki, A. Kuramata, T. Masui, and S. Yamakoshi, Phys. Stat. Solidi A **211**, 21 (2014).
[4]O. Ueda, N. Ikenaga, K. Koshi, K. Iizuka, A. Kuramata, K. Hanada, T. Moribayashi, S. Yamakoshi, and M. Kasu, Jpn. J. Appl. Phys., Part 1 **55**, 1202BD (2016).
[5]M. J. Tadjer, N. A. Mahadik, V. D. Wheeler, E. R. Glaser, L. Ruppalt, A. D. Koehler, K. D. Hobart, C. R. Eddy, Jr., and F. J. Kub, ECS J. Solid State Sci. Technol. **5**, P468 (2016).
[6]J. Kim, S. Oh, M. Mastro, and J. Kim, Phys. Chem. Chem Phys. **18**, 15760 (2016).
[7]A. M. Armstrong, M. H. Crawford, A. Jayawardena, A. Ahyi, and S. Dhar, J. Appl. Phys. **119**, 103102 (2016).
[8]Z. Galazka, R. Uecker, D. Klimm, K. Irmscher, M. Naumann, M. Pietsch, A. Kwasniewski, R. Bertram, S. Ganschow, and M. Bickermann, ECS J. Solid State Sci. Technol. **6**, Q3007 (2017).
[9]M. Baldini, M. Albrecht, A. Fiedler, K. Irmscher, R. Schewski, and G. Wagner, ECS J. Solid State Sci. Technol. **6**, Q3040 (2017).
[10]S. Rafique, L. Han, M. J. Tadjer, J. A. Freitas Jr, N. A. Mahadik, and H. Zhao, Appl. Phys. Lett. **108**, 182105 (2016).
[11]S. W. Kaun, F. Wu, and J. S. Speck, J. Vac. Sci. Technol. A **33**, 041508 (2015).
[12]M. Higashiwaki, K. Sasaki, H. Murakami, Y. Kumagai, A. Koukitu, A. Kuramata, T. Masui, and S. Yamakosh, Semicond. Sci. Technol. **31**, 034001 (2016).
[13]K. D. Chabak, N. Moser, A. J. Green, D. E. Walker, Jr., S. E. Tetlak, E. Heller, A. Crespo, R. Fitch, J. P. McCandless, K. Leedy, M. Baldini, G. Wagner, Z. Galazka, X. Li, and G. Jessen, Appl. Phys. Lett. **109**, 213501 (2016).

[14]A. J. Green, K. D. Chabak, E. R. Heller, R. C. Fitch, Jr., M. Baldini, A. Fiedler, K. Irmscher, G. Wagner, Z. Galazka, S. E. Tetlak, A. Crespo, K. Leedy, and G. H. Jessen, IEEE Electron Dev. Lett. **37**, 902 (2016).
[15]M. H. Wong, K. Sasaki, A. Kuramata, S. Yamakoshi, and M. Higashiwaki, IEEE Electr. Dev. Lett. **37**, 212 (2016).
[16]K. Sasaki, M. Higashiwaki, A. Kuramata, T. Masui, and S. Yamakoshi, IEEE Electron. Dev. Lett. **34**, 493 (2013).
[17]M. H. Wong, K. Sasaki, A. Kuramata, S. Yamakoshi, and M. Higashiwaki, Appl. Phys. Lett. **106**, 032105 (2015).
[18]S. Oh, G. Yang, and Jihyun Kim, ECS J. Solid State Sci. Technol. **6**, Q3022 (2017).
[19]W. S. Hwang, A. Verma, H. Peelaers, V. Protasenko, S. Ruvimov, H. (Grace) Xing, A. Seabaugh, W. Haensch, C. Van de Walle, Z. Galazka, M. Albrecht, R. Fornari, and D. Jena, Appl. Phys. Lett. **104**, 203111 (2014).
[20]S. Ahn, F. Ren, J. Kim, S. Oh, Jihyun Kim, M. A. Mastro, and S. J. Pearton, Appl. Phys. Lett. **109**, 062102 (2016).
[21]K. Sasaki, M. Higashiwaki, A. Kuramata, T. Masui, and S. Yamakoshi, Appl. Phys. Express **6**, 086502 (2013).
[22]T. Oshima, T. Okuno, N. Arai, Y. Kobayashi, and S. Fujita, Jpn. J. Appl. Phys. **48**, 040208 (2009).
[23]S. Ohira and N. Arai, Phys. Status Solidi C **5**, 3116 (2008).
[24]H. Liang, Y. Chen, X. Xia, C. Zhang, R. Shen, Y. Liu, Y. Luo, and G. Du, Mater. Sci. Semicond. Process **39**, 582 (2015).
[25]J. E. Hogan, S. W. Kaun, E. Ahmadi, Y. Oshima, and J. S. Speck, Semicond. Sci. Technol. **31**, 065006 (2016).
[26]X. Cao, S. J. Pearton, G. T. Dang, A. P. Zhang, F. Ren, and J. M. Van Hove, IEEE Trans. Electron. Dev. **47**, 1320 (2000).
[27]M. Mohamed, K. Irmscher, C. Janowitz, Z. Galazka, R. Manzke, and R. Fornari, Appl. Phys. Lett. **101**, 132106 (2012).
[28]Shihyun Ahn, F. Ren, L. Yuan, S. J. Pearton, and A. Kuramata, ECS J. Solid State Sci. Technol. **6**, P68 (2017).
[29]K. Ip, K. Baik, M. E. Overberg, E. S. Lambers, Y. W. Heo, D. P. Norton, S. J. Pearton, F. Ren, and J. M. Zavada, Appl. Phys. Lett. **81**, 3546 (2002).
[30]C. Steinbruchel, Appl. Phys. Lett. **55**, 1960 (1989).
[31]K. Pelhos, V. M. Donnelly, A. Kornblit, M. L. Green, R. B. Van Dover, L. Manchanda, and E. Bower, J. Vac. Sci. Technol. A **19**, 1361 (2001).
[32]C. C. Chang, K. V. Guinn, I. P. Herman, and V. M. Donnelly, J. Vac. Sci. Technol. A **13**, 1970 (1995).
[33]S. M. Sze and K. K. Ng, *Physics of Semiconductor Devices*, 3rd ed. (John Wiley & Sons, Hoboken, 2007), Chap. 3.
[34]W. Mönch, *Electronic Properties of Semiconductor Interfaces* (Springer, Berlin, 2004).
[35]see, for example, S. W. Pang, in *Handbook of Advanced Plasm Processing Techniques*, edited by R. J. Shul and S. J. Pearton (Springer, Berlin, 2000), Chapter 8.
[36]X. A. Cao, H. Cho, S. J. Pearton, G. T. Dang, A. P. Zhang, F. Ren, R. J. Shul, L. Zhang, R. Hickman, and J. M. Van Hove, Appl. Phys. Lett. **75**, 232 (1999).
[37]T. Oishi, Y. Koga, K. Harada, and M. Kasu, Appl. Phys. Express **8**, 031101 (2015).